SFCVQ and EZW coding method based on Karhunen-Loeve transformation and integer wavelet transformation

Jingwen Yan (闫敬文)[1,2] and Jiazhen Chen (陈嘉臻)[2]

[1]*Department of Electronic Engineering, Shantou University, Shantou 515063*

[2]*Department of Electronic Engineering, Xiamen University, Xiamen 361005*

Received August 16, 2006

A new hyperspectral image compression method of spectral feature classification vector quantization (SFCVQ) and embedded zero-tree of wavelet (EZW) based on Karhunen-Loeve transformation (KLT) and integer wavelet transformation is represented. In comparison with the other methods, this method not only keeps the characteristics of high compression ratio and easy real-time transmission, but also has the advantage of high computation speed. After lifting based integer wavelet and SFCVQ coding are introduced, a system of nearly lossless compression of hyperspectral images is designed. KLT is used to remove the correlation of spectral redundancy as one-dimensional (1D) linear transform, and SFCVQ coding is applied to enhance compression ratio. The two-dimensional (2D) integer wavelet transformation is adopted for the decorrelation of 2D spatial redundancy. EZW coding method is applied to compress data in wavelet domain. Experimental results show that in comparison with the method of wavelet SFCVQ (WSFCVQ), the method of improved BiBlock zero tree coding (IBBZTC) and the method of feature spectral vector quantization (FSVQ), the peak signal-to-noise ratio (PSNR) of this method can enhance over 9 dB, and the total compression performance is improved greatly.

OCIS codes: 100.2000, 100.3010, 300.6320.

A number of compression algorithms have been proposed for hyperspectral images[1−3]. Some algorithms focus on the three-dimensional (3D) transformation, such as 3D integer wavelet transformations (IWTs)[4] and efficient adaptive 3D Karhunen-Loeve transformation (KLT)[5]. These compression ways are suitable for 3D image compression. However, the processing of the 3D transforming, quantizing and coding is too intricacy. What is more, the computing time is increasing with the number of spectral bands growing. These algorithms are hard to implement in hardware. Some recent algorithms typically focused on applying a one-dimensional (1D) KLT along the spectral dimension and subsequently a two-dimensional (2D) image compression method applied to 2D spatial dimensions. In Ref. [6], the KLT/wavelet transform (WT)/embedded zero-tree wavelet (EZW) compression method is reported. The method of EZW has the advantage of easy parallel processing in hardware and the controlled compression rate or distortion rate. Therefore, EZW has been widely used in video and image data compression[7]. Whereas the first generation wavelet base is constructed by translation and dilation[8], the computing process has wasted a large amount of computing and store units. Along with the study of the wavelet theory, Sweldens presented the lifting scheme, a simple construction of second generation wavelets, which need not necessarily to translate and dilate a fixed function[8−10]. Integer wavelet is one kind of the second generation wavelet and is faster than the first generation wavelet implemented in real time. Spectral feature classification vector quantization (SFCVQ) and wavelet SFCVQ (WSFCVQ) had been studied in Ref. [9,11].

In the 1990s, Sweldens of the Bell Labs presented one way to construct the wavelet filter with lifting scheme[8]. Signal is split into two sets, which are not intersectant: even subscript sampling and odd subscript sampling. Considering the relativity of the two sets, the prediction P can well rebuild one set from another set. In order to hold the integrity of the raw data, the next two even sampling values are used to predict the odd sampling value and note down the difference value. Each WT needs two steps to build. At first, the wavelet coefficient needs

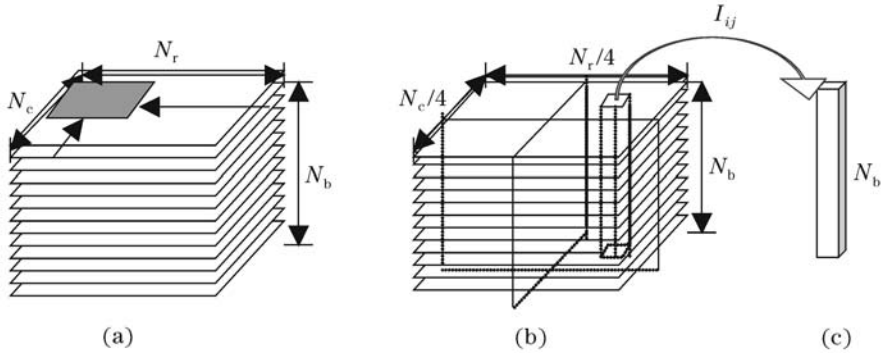

Fig. 1. Vector-constructed and compressed diagram for imaging spectral data by KLT/IWT. (a) Data compression by KLT; (b) subimage spectrum by IWT; (c) a spectral vector of random dot in space.

 © 2007 Chinese Optics Letters

computing, then lifting the down sampling coefficient is proceeded.

Hyperspectral data include a lot of substantial information on the ground. After the data are transformed by KLT/IWT, the compressed hyperspectral information is shown in Figs. 1(a) and (b). Figure 1(c) shows a hyperspectral vector compressed by KLT and IWT in any spatial position point (i, j).

One hyperspectral image consists of $N_{\rm c} \times N_{\rm r}$ pixels in spatial dimensions, and $I_{i,j}(k)$ is spectral information corresponding to a spatial pixel in any position $(k = 1, 2, \cdots, N_{\rm b})$. Thus a vector in $N_{\rm b}$ spectral dimension $I_{i,j}(k)$ is constituted corresponding to a pixel in spatial position

$$I_{i,j} = [I_{i,j}(1), I_{i,j}(2), \cdots, I_{i,j}(N_{\rm b})]^{\rm T}. \quad (1)$$

Because substance is limited in the ground, the hyperspectral vector is finite. We can transfer a hyperspectral vector of $N_{\rm b}$ dimension $Y^{\rm a}_{i,j}$ into an N_b bit binary code corresponding to amplitude changing $Y^{\rm ab}_{i,j}$,

$$Y^{\rm a}_{i,j} = \left[Y^{\rm a}_{i,j}(1), Y^{\rm a}_{i,j}(2), \cdots, Y^{\rm a}_{i,j}(N_{\rm b})\right]^{\rm T},$$
$$(i = 1, 2, \cdots, N_{\rm r}; \quad j = 1, 2, \cdots, N_{\rm c}), \quad (2)$$

$$Y^{\rm ab}_{i,j}(\lambda) = \begin{cases} 1 & \left[Y^{\rm a}_{i,j}(\lambda) - \mu_{i,j} \geq 0\right] \\ 0 & \left[Y^{\rm a}_{i,j}(\lambda) - \mu_{i,j} < 0\right] \end{cases},$$
$$\lambda = 1, 2, \cdots, N_{\rm b}, \quad (3)$$

$$\mu_{i,j} = \frac{1}{N_{\rm b}} \sum_{\lambda=1}^{N_{\rm b}} Y^{\rm a}_{i,j}(\lambda),$$
$$i = 1, 2, \cdots, N_{\rm r}; \quad j = 1, 2, \cdots, N_{\rm c}, \quad (4)$$

and $Y^{\rm s}_{i,j}$ is an $N_{\rm b} - 2$ bit binary code of slope variety, which can be represented by

$$Y^{\rm s}_{i,j} = \left[Y^{\rm s}_{i,j}(1), Y^{\rm s}_{i,j}(2), \cdots, Y^{\rm s}_{i,j}(N_{\rm b})\right]^{\rm T},$$
$$i = 1, 2, \cdots, N_{\rm r}; \quad j = 1, 2, \cdots, N_{\rm c}, \quad (5)$$

$$Y^{\rm s}_{i,j}(\lambda) = \begin{cases} 1 & \left[I_{i,j}(\lambda + 1) - I_{i,j}(\lambda - 1) \geq 0\right] \\ 0 & \left[I_{i,j}(\lambda + 1) - I_{i,j}(\lambda - 1) < 0\right] \end{cases},$$
$$\lambda = 1, 2, \cdots, N_{\rm b}. \quad (6)$$

Then $Y^{\rm s}_{i,j}$ and $Y^{\rm ab}_{i,j}$ are combined into a binary code $Y_{i,j}$

$$Y_{i,j} = Y^{\rm ab}_{i,j} Y^{\rm s}_{i,j}, \quad i = 1, 2, \cdots, N_{\rm r}; \quad j = 1, 2, \cdots, N. \quad (7)$$

A $2(N_{\rm b} - 1)$ bit binary code is shorter than the original hyperspectral vector. Code matching is proceeded in binary bit. Hamming range is applied to measure the similarity of two codes. By the coding process, the coding method will produce error in decoding. In order to enhance compression performance, a scalar quantization coding will be applied. This measure will add a bit to lead to low compression rate. Without adding standard normal character bit[9], an improvement way of block truncated coding (BTC) is used. $N_{\rm b}$ pixels in the spectral dimension are encoded when BTC is proceeded, and a same method can transfer hyperspectral data to a binary code. The mean value vector $Y^{\rm ab}_{i,j}$ is computed, the block is divided into 1 and 0 subblocks according to the mean value, and the two subblock mean values, E_1 and E_0, are computed.

The system block diagrams used in this paper are shown in Fig. 2. The first step is the orthogonal transformation of the hyperspectral data, which can eliminate the relativity among all bands. The second step is the IWT, SFCVQ and EZW are used to compress data after the KLT and IWT.

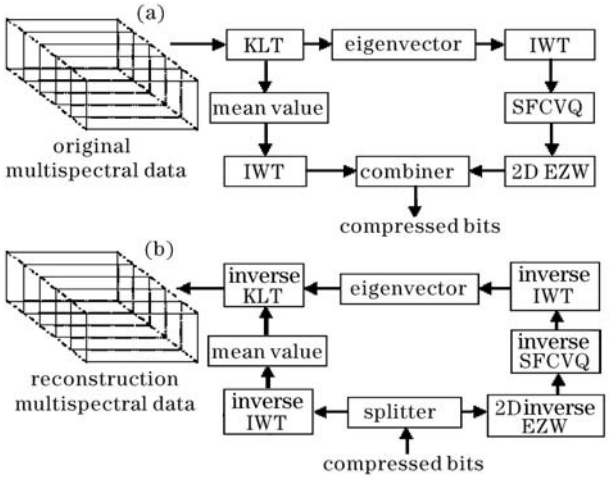

Fig. 2. (a) Coding procedure and (b) decoding procedure diagrams of hyperspectral compression system.

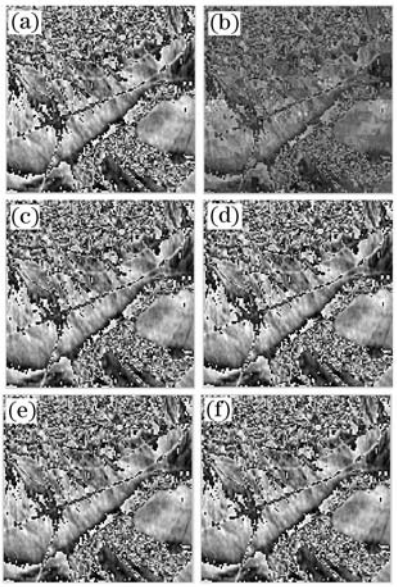

Fig. 3. 61st band spectral image compression results. (a) Original image; (b) first wavelet transformation, PSNR = 30.9847 dB, compression rate 0.14048; (c)—(f) S + P IWT, CDF97 IWT, LS97 IWT, (5,3) IWT, PSNR = 35.4557 dB, compression rate 0.054755.

Table 1. Comparison of the Different Compression Methods

Compression Method	KLT/WT/WSFCVQ	KLT/WT/IBBZTC	KLT/WT/FSVQ	KLT/IWT/EZW
PSNR (dB)	24	16	20	35.45

We use KLT to compress the 224 bands of the hyperspectral image. At each time, we get 8×8 sub-pictures out of each dimension to form a spectral image set of $8 \times 8 \times 224$. Then KLT is used on this image set. Afterwards, the size of the result matrix is $64 \times 64 \times 256$.

The first wavelet transformation, S + P IWT, CDF97 IWT, LS97 IWT and (5,3) IWT are used in hyperspectral image compression as shown in Fig. 3. After that, the EZW is used for scanning five times to compress hyperspectral image. From our experimental results, we can conclude as follows. 1) The compression result of the first generation WT is no better than the second generation WT, under the condition of 3 times wavelet decomposing and 5 times EZW scanning. 2) Considering different effects of hyperspectral data in the same space, we get a higher compression performance using the given method. Figure 4 is the curve error comparison of different spectral bands in the same space (64, 64) between the first WT and the S + P WT, and implies that the error fluctuating extent of the first generation WT is 1.5 times bigger than the second generation WT, under the condition of same wavelet decomposition times and encoding scanning times. 3) Under the condition of some peak signal-to-noise ratio (PSNR), the method can improve 9 dB in comparison with wavelet SFCVQ (WSFCVQ), FSVQ and IBBZTC. 4) From Table 1, it is obviously pointed out that IWT can realize higher PSNR and faster arithmetic speed, on the background that the same compression ratio is 240.

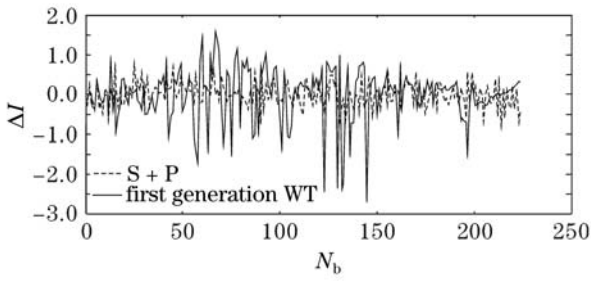

Fig. 4. Curve error comparison of different spectral bands in the same space (64, 64) between the first WT and the S + P WT.

This work was supported by the National Natural Science Foundation of China (No. 60472081), the Avigation Science Foundation (No. 05F07001), and the 985 Innovation Project on Information Technique of Xiamen University (2004—2007). J. Yan's e-mail address is yjwen@xmu.edu.cn.

References

1. Y. Li, C. Wu, J. Chen, and L. Xiang, Acta Opt. Sin. (in Chinese) **21,** 691 (2001).
2. J. Yan, H. Sun, and S. Zhang, Optics and Precision Engineering (in Chinese) **5,** 30 (1997).
3. L. Zhang, L. Huang, and W. Zhao, Optics and Precision Engineering (in Chinese) **14,** 108 (2006).
4. J. E. Fowler and D. N. Fox, IEEE Trans. Geoscience and Remote Sensing **39,** 284 (2001).
5. L. Chang, C.-M. Cheng, and T.-C. Chen, in *Proceedings of 4th IEEE Southwest Symposium on Image Analysis and Interpretation* 252 (2000).
6. J. Yan, G. Shen, X. Hu, and F. Xu, Acta Opt. Sin. (in Chinese) **22,** 691 (2002).
7. J. Yan and A. Zhou, Acta Electron. Sin. (in Chinese) **22,** 834 (2002).
8. W. Sweledens, SIAM J. Math Anal. **29,** 511 (1997).
9. S. Chen, L. Huang, and J. Guo, Optics and Precision Engineering (in Chinese) **14,** 198 (2006).
10. C. Qian, Z. Liu, D. Liu, and K. Zhao, Computer Engineering and Applications (in Chinese) **23,** 89 (2004).
11. J. Yan, G. Shen, X. Hu, and F. Xu, Acta Opt. Sin. (in Chinese) **23,** 1163 (2003).
12. J. Yan, G. Shen, X. Hu, and F. Xu, J. Remote Sensing **4,** 290 (2000).